NEAR-SURFACE ICE LIKELY CAUSE OF THERMAL ANOMALY IN MARTIAN NORTH POLAR ERG.

N. E. Putzig[1], M. T. Mellon[2], K. E. Herkenhoff[3], R. J. Phillips[1], B. J. Davis[1], and K. J. Ewer[4]. [1]Southwest Research Institute, Planetary Science Directorate, Boulder, CO (contact: nathaniel@putzig.com); [2]University of Colorado, Laboratory for Atmospheric and Space Physics, Boulder, CO; [3]United States Geological Survey, Astrogeology Team, Flagstaff, AZ; [4]Embry-Riddle Aeronautical University, Prescott, AZ.

Introduction: Previous investigations of Mars' north polar erg report values of thermal inertia much lower than expected for typical dune-forming sand. To account for the thermal anomaly, sand-sized agglomerations of dust were proposed as the primary constituent of the erg. Here, we use a wider range of thermal observations and conduct forward modeling of heterogeneity to find that near-surface layering of normal basaltic sand over shallow ground ice is sufficient to explain the thermal behavior of the erg, obviating the need to invoke more exotic materials.

Background: Several features in the polar regions of Mars hold clues to its past and present global climate. Most prominently, the layered deposits are believed to be largely composed of water ice and to result from cyclical climate variations over a broad range of time scales [1,2]. After seasonal CO_2 frosts sublimate, the northern layered deposits remain capped by bright residual water ice and surrounded by a dark annulus (Fig. 1a) of dune-forming materials known as the polar erg. Neutron data indicate that water ice is also present within a meter of the erg's surface [3]; such ice may provide additional constraints on climate.

The color, low albedo, and dune morphology of the polar erg are similar to those of dunes seen at lower latitudes [4] and interpreted as sand-sized basaltic materials [5,6,7], with up to 30 wt% gypsum [8]. While the lower-latitude dunes exhibit intermediate thermal inertia (~250 tiu, where tiu = J m^{-2} K^{-1} $s^{-1/2}$) consistent with sand-sized grains, the values reported for the polar erg are much lower (~75 tiu). This result has been interpreted to require that the erg materials be much finer grained [9,10]. Bonding of fines into larger, low-density aggregate particles that are capable of forming dunes [11,12] has been widely accepted as a solution to the thermal discrepancy. Presumably, the agglomeration occurs when the dust is weathered out of the layered deposits [1,2,12], and the sand-sized composite grains are then transported within the erg by saltation. Recent studies associate the dune materials to a newly identified unit at the base of the layered deposits [13,14].

Thermal inertia and heterogeneity: Modeling studies show that surface heterogeneity may cause anomalous thermal behavior [15,16], allowing an alternative explanation for the thermal properties of the erg. Rather counterintuitively, certain configurations of near-surface layering can produce values of apparent thermal inertia (as derived when assuming constant properties) that are substantially lower than the intrinsic thermal inertia of both the surface layer and its substrate [16]. Thus, the polar erg may be surfaced by ordinary basaltic sand, with its low apparent thermal inertia attributable to an effect of surface heterogeneity from the icy substrate.

Globally, diurnal and seasonal variations in apparent thermal inertia up to a few hundred tiu indicate that heterogeneity is a major factor in the thermal behavior of the Martian surface, and the polar regions show thermal characteristics that are broadly

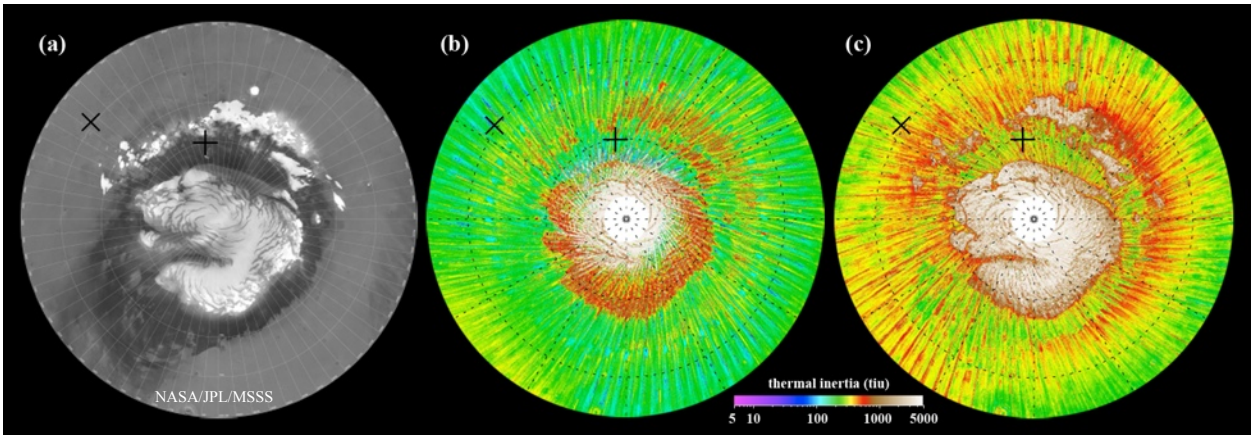

Figure 1. North polar region, 65–90°N, 0°W at bottom. (a) Mosaic of MOC wide-angle images; polar erg is the irregular, dark material surrounding bright layered deposits. (b, c) Annual-median apparent thermal inertia near (b) 2AM and (c) 2PM as derived from TES observations [17]. Orbit-track-aligned streaks are due to seasonal variations. × is Phoenix landing site (Fig. 2a). + is center of HiRISE image (Figs. 2b-d, 3) within the erg's Olympia Undae (area of lower thermal inertia at 120-210°W, 78-83°N).

consistent with layered surfaces (Fig. 1b,c) [17]. A key element in this analysis is the use of both nighttime and daytime results, particularly for the polar regions where seasons free of CO_2 ice largely overlap those when the Sun is predominantly above the horizon.

Figure 2a shows a comparison of seasonal MGS TES results with those from models of sand (223 tiu) overlying 'rock' (2506 tiu) at the Phoenix landing site. The rock value is also representative of the ground ice identified at this site by the lander [18]. For models with sand thicknesses approaching or exceeding a diurnal skin depth (1/26 of δ_S, the seasonal skin depth), the 2AM apparent thermal inertia can be substantially less than that of the sand. Thus, one may underestimate the inherent thermal inertia of the surface materials in this scenario if analysis is focused solely on nighttime observations or uses annual-mean values fit to diurnal temperatures (i.e., as was done with Viking data).

Heterogeneity in the polar erg: At the higher latitudes where the polar erg is located, the seasonal range of useful TES data is even more limited than for Phoenix, and seasonal thermal variations are larger (Figs. 2b-d). To resolve the short-term, rapid changes, we remapped the north polar region with a finer seasonal increment of 5° L_S (cf. 10° used in Fig. 2a and globally by [16]). This improvement allows us to discriminate between models having layers or mixtures of various surface materials for matching to the observed thermal behavior (Fig. 2b-d). The best-fitting matches occur for models with an ice-cemented substrate (thermally equivalent to rock) beneath a dry surface layer, and our analysis techniques allow us to constrain the upper-layer thickness within 10 cm or better. We find the results for the erg to be most consistent with a sand layer of ~15-25 cm (Fig. 2b), with dust-layer models yielding poorer fits (Fig 2c).

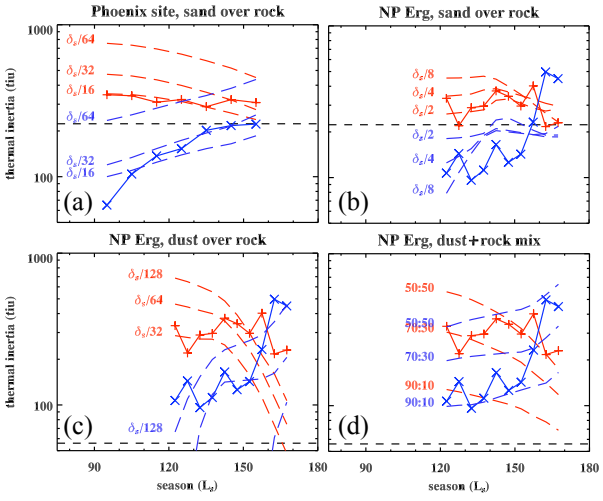

Figure 2. Seasonal 2AM (blue) and 2PM (red) apparent thermal inertia from TES (×, + symbols) and from various models (dashed curves) of sand or dust and rock (i.e., ground ice) at (a) the Phoenix site (× in Fig. 1) and (b-d) in the polar erg (+ in Fig. 1). Horizontal dashed lines represent sand (223 tiu) or dust (56 tiu). Labels in (a-c) are upper-layer thickness in fractional seasonal skin depth, δ_S (70 cm for sand, 21 cm for dust). Labels in (d) are dust:rock mixing ratio. Models in (a) and (b) provide the best fits, with ~4 cm and ~20 cm of sand at Phoenix and at the erg site, respectively. Next-best models of dust-rock (c) layering and (d) mixing have larger deviations from the TES results and are not favored here. L_S ranges are limited by transient CO_2 frost.

For some geometries, horizontal heterogeneity may have thermal behavior similar to that of layering [16]. In the erg, MRO HiRISE images show bright deposits between individual dune crests (Fig. 3), which may be relatively consolidated and thus of higher thermal inertia. However, the best-fitting models of this type (70:30 mixture of dust and rock; Fig. 2d) do not adequately capture the observed thermal behavior.

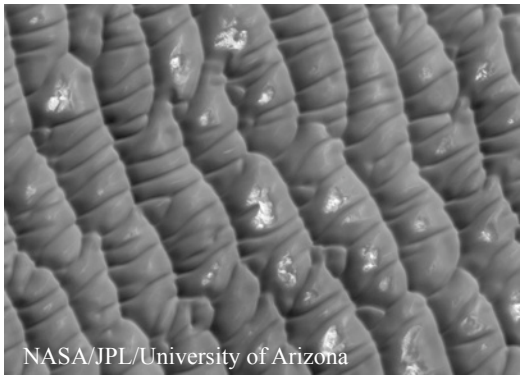

Figure 3. Portion of HiRISE image PSP_001736_2605 (center at 80.19°N, 168.77°W; + in Fig. 1), showing an area in the Olympia Undae region with bright deposits between dune crests. Illumination is from lower left. Image is 4.6 km wide.

References: [1] Thomas P. et al. (1992) in: *Mars*, Kieffer H.H. et al. (1992) U. AZ Press. [2] Clifford S.M. et al. (2000) *Icarus 144*, 210–242. [3] Feldman W.C. et al. (2008) *Icarus* 196, 422-432. [4] Thomas P. & Weitz C. (1989) *Icarus 81*, 185-215. [5] Sagan C. & Bagnold R.A. (1975) *Icarus 26*, 209-218. [6] El-Baz F. et al. (1979) *JGR 84*, 8205-8221. [7] Breed C.S. et al. (1979) *JGR 84*, 8183-8204. [8] Horgan et al. (2009) *JGR* 114, E01005. [9] Paige D.A. et al. (1994) *JGR 99*, 25,959–25,991. [10] Vasavada A.R. et al. (2000) *JGR 105*, 6961–6969. [11] Herkenhoff K.E. & Vasavada A.R. (1999) *JGR 104*, 16,487–16,500. [12] Cutts J.A. et al. (1976) *Science 194*, 1329-1337. [13] Byrne S. & Murray B.C. (2002) *JGR 107*, E6, 5044. [14] Fishbaugh K.E. & Head J.W. (2005) *Icarus 174*, 444-474. [15] Putzig N.E. & Mellon M.T. (2007) *Icarus 191*, 52-67. [16] Mellon M.T. & Putzig N.E. (2007) *LPS XXXVIII*, Abstract #2184. [17] Putzig N.E. & Mellon M.T. (2007) *Icarus 191*, 68-94. [18] Mellon M.T. et al., *JGR*, doi:10.1029/2009JE003417, in press.